Chapter 8

REACTION KINETICS

In this chapter, we will discuss the time evolution of simple reactions in reduced spatial dimension. Diffusion-limited reactions have played an important role in the development of nonequilibrium statistical physics. Such processes are extremely simple to formulate, their numerical implementation is straightforward, yet they reveal rich phenomenology. Because of their simplicity, some basic features of diffusion-limited reactions can be obtained by scaling and dimensional analysis arguments, as mentioned in Chapter 1. For the purposes of this book, our main interest is in presenting methods of exact solution. These have almost exclusively been developed for the simplest reactions in one dimension. These analytical approaches provide a nice demonstration of the important role of fluctuations in low-dimensional systems.

The reactions that we will study contain three basic ingredients—the reaction itself, the transport mechanism, and (potentially) the input of reactants. We study the limit where reaction occurs immediately when reactants meet. Thus the reaction is controlled by this rate of encounters—the *diffusion-controlled* limit. In contrast, in the *reaction-controlled* limit, reactants must meet many times before a reaction actually occurs. The former case is simpler to treat and is physically more interesting. In this chapter, we will investigate the following prototypical reactions:

- Single-species annihilation among identical reactants, $A + A \to 0$.
- Coalescence, $A + A \to A$, where two reactants merge into one upon an encounter, with the product being identical in nature to the initial particles.
- Aggregation, $A_i + A_j \to A_{i+j}$. Chapter 3 treated the rich behavior of this reaction in the mean-field limit. Here we will discuss this reaction in one dimension.
- Two-species annihilation, $A + B \to 0$. Here A's and B's are non-interacting among themselves, but different species annihilate when they meet.

A tacit assumption in all these reaction is that diffusion is the transport mechanism that brings reactants together. While we will mostly consider this physically-relevant situation, we will also investigate examples where the particles move along constant-velocity trajectories—so-called ballistic reactions. Another important physical attribute of the reactions listed above is their irreversibility. While the simplest situation for theoretical analysis are irreversible reactions, we will also study the role of external input and reversibility on some of these reactions.

8.1 Annihilation $A + A \to O$

Irreversible reaction

Perhaps the most elementary reaction is single-species annihilation, $A + A \to O$. It is convenient to consider this reaction when the reactants live on the sites of a regular d-dimensional lattice. Initially, the reactant density is c_0 and we allow each site to be occupied by at most one particle. Particles hop to a nearest-neighbor site with a constant rate, set to 1/2. When the destination site is occupied, annihilation occurs.

Annihilation occurs with rate 1, twice the rate of hopping, because either of the two neighboring particles may hop. These hopping and annihilation events are illustrated in Figure 8.1 for one dimension.

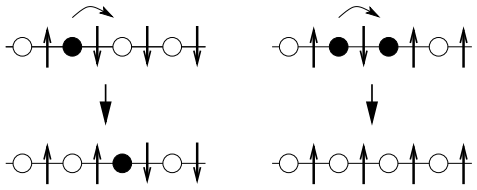

Figure 8.1: Single-species annihilation on a one-dimensional lattice: (left) hopping to an empty site with rate 1/2 and (right) annihilation with rate 1. Also shown is an equivalent representation in terms of Ising spins, where a pair of oppositely-oriented spins is equivalent to an intervening domain wall particle.

The reason why this problem in one dimension is so simple is is that Glauber unknowingly already solved the problem! Let's recall our discussion in Sec. 6.2 of the $T = 0$ Ising model that is endowed with single spin-flip dynamics. Transitions that raise the energy are forbidden, while energy-lowering transition occur with rate 1, and energy-conserving transitions occur with rate 1/2. Identifying domain walls in the spin system with particles in the reaction, the two problems are identical (Fig. 8.1). Formally, the occupation number $n_i = 1$ or 0, that indicates whether a site is occupied or empty, is obtained from the corresponding spin configuration on the dual lattice via the transformation $n_i = (1 - s_i s_{i+1})/2$.

For simplicity, let's consider the completely occupied initial condition, $c(0) = 1$, corresponding to the antiferromagnetic initial condition in the equivalent spin system. From (6.39), the particle concentration c is (after identifying the particle concentration with the domain wall density $\equiv \rho$)

$$c(t) = I_0(2t)e^{-2t}. \tag{8.1}$$

From the asymptotics of the Bessel function, the concentration decays as

$$c(t) \simeq (4\pi t)^{-1/2}, \tag{8.2}$$

as $t \to \infty$. An intuitive way to obtain this result is to note that an isolated random-walk particle typically visits a region of size $x \sim t^{1/2}$ after a time t. when annihilation occurs, the number of particles that can remain within this length scale must be of the order of 1; if there were more particles in this region, they would have annihilated previously. Thus the typical spacing between particles is of the order of this diffusive length scale, and the concentration is the inverse of this scale. An important feature of this argument and also of the exact result is that the asymptotic density does not depend on the initial density.

Closely related to the particle density is the distribution of voids between particles. Using the nomenclature of chapter 5, a void of length n consists of n successive empty sites that is terminated at both ends by an occupied site. Let V_n be the distribution of voids of size n between two successive particles. Since the density decays as $t^{-1/2}$, the typical void length should grow as $t^{1/2}$. We therefore expect that the distribution of void lengths will depend only on the ratio of the length of a void to the typical void length. Consequently, the void length distribution should have the self-similar form

$$V_n(t) \simeq t^{-1}\Phi(nt^{-1/2}). \tag{8.3}$$

The time-dependent prefactor follows from the condition $\sum V_n \propto t^{-1/2}$. We can then use physical reasoning to find the asymptotic behavior of $\Phi(z)$. The density of minimal-size voids, those of length 0, is related to the density decay by $V_0 = -dc/dt \sim t^{-3/2}$. This asymptotic behavior is consistent with the above scaling form for V_n when the scaling function has the asymptotic behavior $\Phi(z) \sim z$ for $z \to 0$. This behavior is precisely what we found in the analysis of the void-size distribution for the zero-temperature Ising-Glauber model in Sec. 6.2. In addition to the linear vanishing of small-length voids, we also found that the void density decays exponentially at large distances

$$\Phi(z) \sim \begin{cases} z & z \ll 1, \\ e^{-z/z_*} & z \gg 1. \end{cases} \tag{8.4}$$

What happens when the spatial dimension is different than 1? For these physically more relevant cases (especially 2 and 3 dimensions) there is currently no method that gives the exact solution for the density. Instead we must resort to heuristic approaches to obtain the decay of the density for arbitrary spatial dimensions d. When d is greater than an upper critical dimension d_c, mean-field theory provides the correct asymptotic behavior of the density. For single-species annihilation, mean-field theory is the same as the rate equation approximation in which the probability that two particles meet is simply proportional to the square of the density. This approach implicitly assumes spatial homogeneity and that the two-point density can be factorized into a product of single-point densities. When two particles do meet, the rate at which they react is then given by the reaction rate k that was already discussed in chapter 2 and the result for the reaction rate is quoted in Eq. (2.45). Thus for $d > 2$, the density is described by the rate equation

$$\frac{dc}{dt} = -k\, c^2, \tag{8.5}$$

with $\propto Da^{d-2}$, with a the radius of the reactants.

For $d \leq 2$, we simply adapt the rate equation approach by allowing the reaction rate to be time dependent. This time dependence accounts for the fact that nearby random walks are certain to eventually meet when $d < 2$. This means that the local density is depleted close to the surface of any reactant so that the reaction rate should decrease with time. Thus for $d \leq 2$, we write

$$\frac{dc}{dt} = -k(t)\, c^2, \tag{8.6}$$

and then use the time-dependent form for the reaction rate previously given in Eq. (2.45):

$$k(t) \propto \begin{cases} D^{d/2}\, t^{(d-2)/2} & d < 2, \\ 4\pi D/\ln t & d = 2, \\ Da^{d-2} & d > 2. \end{cases} \tag{8.7}$$

Using these results in the rate equation (8.6) then yields the asymptotic decay of the density for all spatial dimensions:

$$c(t) \propto \begin{cases} t^{-d/2} & d < 2, \\ t^{-1} \ln t & d = 2, \\ t^{-1} & d > 2. \end{cases} \tag{8.8}$$

The main point is that the density decays more slowly than that predicted by mean-field theory. This slow decay is yet another manifestation of the depletion zone around each reactant, which slows the overall rate of reaction.

Steady state reaction

It is natural to study the influence of a steady input of reactants on annihilation. The input balances the loss of particles by annihilation so that a steady state is achieved. As we shall discuss, the precise nature of the input has a crucial effect on the long-time behavior. Consequently, the long-time state may actually represent thermodynamic equilibrium or the steady state retains a non-equilibrium character.

Let us first consider the simpler case where a pair of particles are inserted into neighboring sites of the system at a fixed rate h, while the reaction $A + A \to 0$ between nearest-neighbor pairs always occurs at rate 1. Why is adding pairs of particles at a fixed rate than merely adding single particles? To answer this question it is useful to view the annihilation reaction as creating an inert immobile product, that is, $A + A \to I$. The input of a pair is equivalent to the inert product splitting up into the pair of original A particles. Therefore pair input is nearly equivalent to the *reversible* annihilation reaction

$$A + A \leftrightarrow I.$$

There is a small caveat to this equivalence. In the case of pair input, once a pair of particles is created, they may diffuse away from their point of origin, after which an additional pair may then be created at this

same origination point. In the reversible reaction, however, there cannot not be multiple production of pairs from the vacuum, but only the production of a single pair from the breakup of a product particle. Thus the equivalence to the reversible reaction becomes exact in the limit of small input rate.

In the nomenclature of the equivalent system of Ising spins with Glauber kinetics (see Fig. 8.2), the input of a particle pair corresponds to an energy-raising single spin-flip event. Consequently the input of pairs in the annihilation reaction is equivalent to the temperature being finite in the spin system.

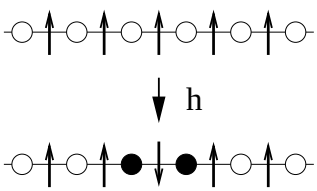

Figure 8.2: Equivalence between the input of a pair of particles at neighboring sites with a rate h and an energy raising event in the Ising-Glauber model.

Since the reaction is equivalent to the finite-temperature Ising-Glauber model, detailed balance is satisfied by construction. We now apply the detailed balance condition to derive the equilibrium density. Since $A + A \to I$ with rate 1 and $I \to A + A$ with rate h, the detailed balance condition is

$$1 \times P(\ldots 11 \ldots) = h \times P(\ldots 00 \ldots),$$

where $P(\ldots n_{i-1}, n_i, n_{i+1} \ldots)$ denotes the probability of the occupany configuration $\{n_i\}$. Next we use the fact that for the Ising model in thermal equilibrium, the energy of each pair of spins is independent of all other spins. Therefore, the distribution of domain walls factorizes into a product over individual domain wall probabilities. Thus the detailed balance condition translates to the equation $c^2 = h(1-c)^2$, where c is the domain wall density. The steady-state density is therefore,

$$c(t) = \frac{h^{1/2}}{1 + h^{1/2}}. \tag{8.9}$$

One can verify that the same result also follows from (6.36) when $h = e^{-\beta}$. The steady-state density (8.9) is obvious *a posteriori* when one realizes that the sites are uncorrelated. The rate of particle gain equals the product of the probability of finding two vacant sites and the creation rate; similarly, the particle loss rate equals the probability of finding two occupied sites times the annihilation rate. These two processes lead to the rate equation $\frac{d\rho}{dt} = -\rho^2 + h(1-\rho)^2$ that again gives the steady-state density (8.9).

The steady state has a markedly different nature when particles are added one at a time

$$O \xrightarrow{h} A. \tag{8.10}$$

If a particle is added to an already occupied site, then annihilation is defined to occur immediately so that the outcome is an empty site. Thus the the process $A \to 0$ also can occur, but its influence is negligible in the interesting limit of $h \to 0$. For this single-particle input, detailed balance cannot be satisfied as there are no processes that play the reverse role of annihilation and of input. Thus the system reaches a steady state with a fundamentally non-equilibrium character.

We can determine the properties of this steady state by the Glauber formalism. When a single particle is created with rate h, the occupation n_i at the i^{th} site changes from 0 to 1. This single-particle creation corresponds to flipping all spins right of the i^{th} bond (Fig. 8.3), that is,

$$\ldots s_{i-1}, s_i, s_{i+1}, s_{i+2} \ldots \xrightarrow{h} \ldots s_{i-1} s_i, -s_{i+1}, -s_{i+2} \ldots. \tag{8.11}$$

Thus whenever a particle is added at the i^{th} with $1 \le i \le k$, all the spins s_j with $j > i$ also flip and the product $g_k = s_0 s_k$ changes sign. Therefore $g_k(t + \Delta t) = g_k(t)$ with probability $1 - (hk)\Delta t$ and $g_k(t + \Delta t) = -g_k(t)$ with probability $hk\Delta t$. The rate of change in the correlation function $G_k = \langle g_k \rangle$ due to the process (8.11)

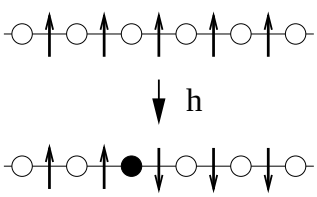

Figure 8.3: Equivalence between the input of a single with a rate h and a non-local energy raising event in the Ising-Glauber model in which all spins to the right of the domain wall flip.

equals $-2hkG_k$. Adding this term to the master equation for the correlation function of the Ising-Glauber model Eq. (6.36), that also describes irreversible single-species annihilation, then gives

$$\frac{dG_k}{dt} = -2(1+kh)G_k + G_{k-1} + G_{k+1} \tag{8.12}$$

for $k \geq 1$. The boundary condition is $G_0 = 1$.

In the steady state, the pair correlation function obeys

$$2(1+kh)G_k(h) = G_{k-1}(h) + G_{k+1}(h). \tag{8.13}$$

Eq. (8.13) closely resembles the following recursion relation for the Bessel function of the first kind

$$\frac{2\nu}{x} J_\nu(x) = J_{\nu-1}(x) + J_{\nu+1}(x). \tag{8.14}$$

We can match this recursion with (8.13) be setting $\frac{2\nu}{x} = 2(1+kh)$. This defines a one-parameter family of relations that connect (k,h) with (ν, x). A simple choice is $x = h^{-1}$ and $\nu = k + h^{-1}$, which then gives for the pair correlation function for $k \geq 0$,

$$G_k(h) = C\, J_{k+h^{-1}}(h^{-1}); \tag{8.15}$$

the prefactor $C = 1/J_{h^{-1}}(h^{-1})$ ensures the normalization $G_0 = 1$.

In the small-input limit, we make use of the asymptotic behavior of the Bessel function

$$J_\nu(\nu + x\nu^{1/3}) \sim (2/\nu)^{1/3} \mathrm{Ai}(-2^{1/3}x), \tag{8.16}$$

with $\mathrm{Ai}(x)$ the Airy function, to rewrite the particle density as

$$c = \frac{1}{2}(1 - G_1) \sim \frac{1}{2}\left[1 - \frac{\mathrm{Ai}((2h)^{1/3})}{\mathrm{Ai}(0)}\right]. \tag{8.17}$$

Expanding the Airy function to first order for small h, we obtain

$$c \sim 2^{-2/3}\, \frac{\mathrm{Ai}'(0)}{\mathrm{Ai}(0)}\, h^{1/3} \approx 0.4593\, h^{1/3} \tag{8.18}$$

as $h \to 0$. For small h, the density is much larger compared to the $h^{1/2}$ dependence for the case of pair input (see Eq. (8.9)). The increased density for single-particle input arises because of the same spatial correlations between particles that occurs for irreversible annihilation.

The pair correlation function for single-particle input also differs substantially from the equilibrium correlation distribution. For large k, the recursion (8.13) for the correlation function reduces to

$$\frac{\partial^2 G(k)}{\partial k^2} = 2hk\, G(k). \tag{8.19}$$

For large k, this equation may be conveniently solved by using the WKB method and the result is (see highlight):

$$G_k \sim e^{-ak^{3/2}}, \tag{8.20}$$

with the constant $a = (8h/9)^{1/2}$. Thus correlations decay much more quickly with distance than the exponential decay (6.37) of the Ising-Glauber model at equilibrium.

The WKB method

The WKB method is a powerful analysis technique to obtain the asymptotic solution of a differential equation near an irregular singular point. A prominent such example is the equation (8.19), which can be written simply as $y'' = xy$. This equation also arises as the form of the time-independent Schrödinger equation near a classical turning point. At an irregular singular point, the dependence of y is faster than a power law and the standard approach to obtain the solution is to write it as the expansion $y = \exp[\phi_1(x) + \phi_2(x) + \ldots]$ and then solve for the expansion functions ϕ_n recursively. To leading order, we then obtain $(\phi_1')^2 = x$. There are two solutions to this equation, but the correct one is $\phi_1 = -\frac{2}{3}x^{3/2}$ which decays as $x \to \infty$. At the next level of approximation, we then obtain $\phi_2' = -\frac{1}{4}x^{-1}$. This yields the leading behavior

$$y \sim x^{-1/4} \exp\left[-\frac{2}{3}x^{3/2}\right]. \tag{8.21}$$

If one continues this method to the next level of approximation, one finds that all higher-order terms have the form of a vanishing correction to the leading behavior (8.21) as $x \to 0$.

As a counterpoint to the exact analysis given above, let's try to learn what we can about the steady state and the approach to the steady state by applying scaling. In the interesting small-input limit, we expect that the influence of the input will not be felt until the density decays to the point where the input represents a substantial perturbation. Thus for $h \to 0$, we expect that the density will decay as $t^{-1/2}$ in an intermediate-time regime that is large compared to the mean time for reactants to meet by diffusion, but small compared to the time between input events within a typical interparticle separation. However, at long times, the density should become constant. These two limiting behaviors may be encapsulated by the scaling ansatz

$$c(h,t) \sim h^\alpha \Phi(t\, h^\beta) \quad \text{with} \quad \alpha = \begin{cases} 1/3 & \text{pair input,} \\ 1/2 & \text{single-particle input.} \end{cases} \tag{8.22}$$

In this small-time limit, the input can be ignored and the density decays as $c \sim t^{-1/2}$. Assuming that $\Phi(z) \propto z^\gamma$ as $z \to 0$, we must have $\Phi(z) \sim z^{-1/2}$. Consequently, the exponent relation $\beta = 2\alpha$ must be satisfied to eliminate the dependence on the input rate. This reasoning gives

$$\beta = \begin{cases} 1 & \text{pair input,} \\ 2/3 & \text{single-particle input.} \end{cases} \tag{8.23}$$

Thus the relaxation for pair input is substantially slower that in single-particle input.

Finally, we can adapt the rate equation approach to give both the steady state and the time-dependent behavior under the influence of particle input. For pair input (equilibrium), we use the fact neighboring remain uncorrelated, $\frac{d}{dt}c = -c^2 + h$, while for the nonequilibrium steady-state, the effective reaction rate is proportional to the density and $\frac{d}{dt}c = -k(c)c^2 + h$. Using the effective reaction rates this generalizes Eq. (8.18) to arbitrary dimensions

$$c(h) \sim \begin{cases} h^{d/(d+2)} & d < 2, \\ h^{1/2}[\ln h^{-1}]^{1/2} & d = 2, \\ h^{1/2} & d > 2. \end{cases} \tag{8.24}$$

8.2 Coalescence $A + A \to A$

We now study the kinetics of the coalesence reaction $A + A \to A$ in one dimension. It is convenient to again to define the particle to live on the sites of a lattice and that each lattice site may be occupied by at most one particle. Particles hop to nearest neighbor sites with rate 1/2. If the destination site is occupied, the two particles coalesce, with the product having the same characteristics as the two initial particles. These processes can be represented by:

$$AO \xleftrightarrow{1/2} OA, \qquad AA \xrightarrow{1/2} OA \qquad AA \xrightarrow{1/2} AO. \tag{8.25}$$

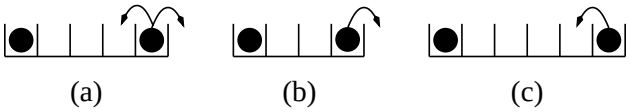

Figure 8.4: Changes in voids of size $n = 3$ due to hopping. Shown are the hopping events that lead to a loss (a) and the two types of gain processes ((b) & (c)).

A convenient way to analyze the coalescence reaction in one dimension is in terms of the voids between neighboring particles. Again, we use the terminology of chapter 5 that a void of length n is a string of n consecutive empty sites with the two sites at the end of the void occupied. The length of a void may either grow or shrink by 1 due to the hopping of a particle at the end of the void (Fig. 8.4). The dynamics of voids are "closed" because a void is affected only by the two particles at its boundary (all other particles are irrelevant!) This closure allows us to write a soluble equation for the void size distribution. Let V_n be the density of voids of size n. As illustrated in Fig. 8.4, the void size performs a random walk and the corresponding master equation for the void size density is (for $n > 0$)

$$\frac{dV_n}{dt} = -2V_n + V_{n+1} + V_{n-1}. \tag{8.26}$$

This equation can be extended to $n = 0$ by noting that the equation for the density of minimal size voids ($n = 0$), $\frac{dV_0}{dt} = -2V_0 + V_1$, can by put into the same form as (8.26) if one imposes the boundary condition $V_{-1} \equiv 0$.

For simplicity, consider the completely filled initial configuration, $V_n(0) = \delta_{n,0}$. As discussed in Sec. 6.2 (see especially Eq. (6.33)), the solution has the form $I_n(2t)e^{-2t}$, with $I_n(x)$ the modified Bessel function of the first kind. To satisfy the boundary condition $V_{-1}(t) = 0$ we use the image method. Thus we initially place a negative image charge of strength -1 at $n = -2$. Then the void density is

$$V_n(t) = [I_n(2t) - I_{n+2}(2t)]\, e^{-2t}. \tag{8.27}$$

We now use the fact that the particle density equals the total void density, $c = \sum_{k=0}^{\infty} V_k(t)$, since there is a one-to-one mapping between particles and voids. Consequently, the particle density is

$$c(t) = [I_0(2t) + I_1(2t)]\, e^{-2t}. \tag{8.28}$$

Asymptotically, the concentration decays algebraically, $c(t) \simeq (\pi t)^{-1/2}$, as in annihilation (see Eq. (8.2)). The amplitude of the asymptotic decay for coalescence is twice that of annihilation because one particle is lost in each coalescence reaction while two particles are lost in each annihilation.

Using the identity $I_{n-1}(x) - I_{n+1}(x) = \frac{2n}{x} I_n(x)$, we may simplify the result (8.27) for the void density to

$$V_n(t) = \frac{n+1}{t}\, I_{n+1}(2t)\, e^{-2t}. \tag{8.29}$$

In the long time limit, the void density becomes self-similar, following the same form (8.3) as in annihilation. This scaling form is consistent with both the typical void size $n \sim t^{1/2}$ and $c \sim t^{-1/2}$. The scaling function is

$$\Phi_{\rm coa}(z) = \sqrt{\frac{2}{\pi}}\, z\, e^{-z^2/2}. \tag{8.30}$$

At large distances, the void distribution has a Gaussian tail modified by an algebraic prefactor. Large voids are much less likely compared with annihilation, where there is an exponential decay. At small distances, the void density vanishes linearly, reflecting the fact that particles are effectively repelling each other. Particles enhance their survival rate by staying away from each other.

The void distribution shows: (i) correlations are generated dynamically and (ii) particle positions are correlated. Fluctuations are significant and must be taken into account because the likelihood of finding two neighboring particles is much smaller than c^2. The emergence of substantial fluctuations is responsible for the failure of the hydrodynamic approach.

Finite-Size Scaling

Often, we can understand long time asymptotics by determining the fate of a finite system. In coalescence, the final state of a finite system of size L is deterministic and consists of one particle. Consequently, the concentration must saturate at $c(L, t \to \infty) = L^{-1}$. We now assume that the time-dependent concentration is self-similar, *i.e.*, we postulate the scaling form

$$c(L,t) \simeq L^{-1}\Phi\left(\frac{L}{\sqrt{Dt}}\right).$$

The long time behavior dictates the scaling function behavior $\Phi(z) \sim 1$ as $z \to 0$. In the complementary limit $z \to \infty$, the behavior should be independent of system size and therefore $\Phi(z) \sim z$, thereby reproducing the asymptotic behavior $c(t) \sim (Dt)^{-1/2}$.

8.3 Aggregation $A_i + A_j \to A_{i+j}$

In aggregation, each site is either vacant or occupied by a cluster of mass i. Clusters hop to nearest-neighbor sites and when the target site is occupied, the aggregation event $A_i + A_j \to A_{i+j}$ occurs. Here A_k denotes a cluster of mass k. Let c_k be the density of clusters of mass k; mass conservation gives $\sum_k kc_k = 1$. We study spatially homogeneous situations with the monodisperse initial condition, $c_k(0) = \delta_{k,1}$. The basic question we want to answer is: what is the cluster mass distribution and how does it evolve in time? For the constant reaction kernel ($K_{ij} = 1$), aggregation is exactly soluble in one dimension by generalizing the empty interval method.

Irreversible reaction

To determine the cluster mass distribution, it is convenient to introduce auxiliary variables that quantify the amount of mass within an interval of a given size. We define Q_n^k as the probability that the total mass contained in n consecutive sites equals k. By construction $\sum_{k=0}^{\infty} Q_n^k = 1$, and the probability that there is no mass in the n interval, Q_n^0 is just the empty interval probability that was first introduced in our discussion of adsorption phenomena in chapter 5; thus $E_n \equiv Q_n^0$. The fundamental cluster mass distribution, namely the probability to have a cluster of mass k is simply the probability that there is a mass k in an interval of length 1; thus $c_k = Q_1^k$.

The feature that makes aggregation soluble is that the interval probabilities Q_n^k evolve according to the very same discrete diffusion equation that also governs the void and the empty interval densities! The derivation, though, is more delicate because of the need to track both the interval length and the mass contained within the interval. We now require the conditional probability $\tilde{Q}_n^k$ that n consecutive sites that contain a total mass k are followed by an empty site. To write the master equation for Q_n^k, we detail the changes in this quantity due to hopping events at the right boundary (8.5). A similar set of contributions arise at the left boundary.

Intervals of size n and mass k are gained (+) and lost (−) with the following rates:

+ The mass in an n-interval is smaller than k and a cluster hops into this interval to make the final mass equal to k. Thus the mass contained in the interval of length $n+1$ must equal k. The rate of this event equals $[Q_{n+1}^k - \tilde{Q}_{n+1}^k]/2$. The difference of the Q's accounts for the probability that a mass k is contained in an interval of length $n+1$ with the last site on the right of this interval being occupied. The factor $1/2$ accounts for this last cluster hopping to the left to create an interval of length n that contains mass k.

+ The interval mass is larger than k and a cluster at the end of the interval hops out so that the final mass equals k. The rate for this event is $[Q_{n-1}^k - \tilde{Q}_{n-1}^k]/2$.

− The interval mass equals k and a cluster hops into it with rate $-[Q_n^k - \tilde{Q}_{n+1}^k]/2$.

− The interval mass equals k and a cluster hops out of it with rate $-[Q_n^k - \tilde{Q}_{n-1}^k]/2$.

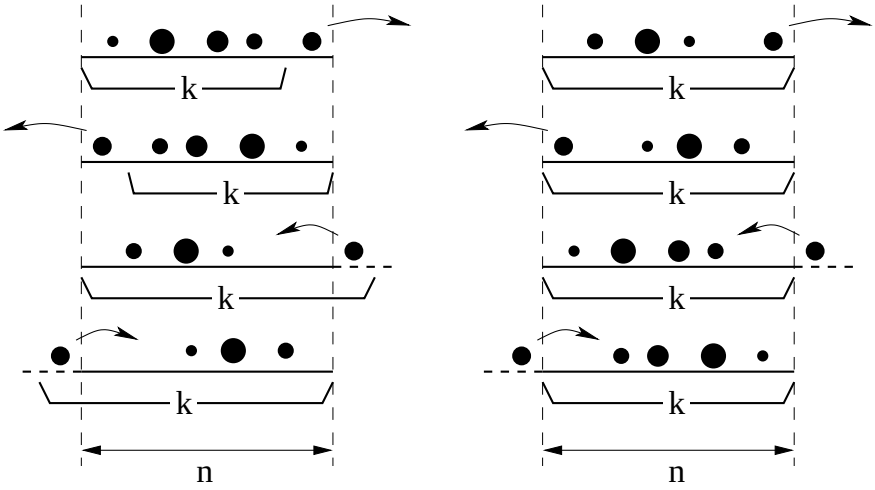

Figure 8.5: Configurations that contribute to the change in the set of states in which a total mass k is contained in an interval of length n. The left-hand side shows the four processes that lead to a gain in Q_n^k, and the right-hand side shows the four loss processes.

Adding all these transition rates, the conditional probabilities miraculously cancel! By including the identical contribution at the second boundary, the evolution of the empty interval density is again described by the discrete diffusion equation

$$\frac{dQ_n^k}{dt} = -2Q_n^k + Q_{n-1}^k + Q_{n+1}^k \tag{8.31}$$

for all $k \geq 0$. The boundary condition is $Q_0^k(t) = 0$ for $k > 0$ (indeed, $E_0 = Q_0^0 = 1$) and we choose the initial condition $Q_n^k(0) = \delta_{n,k}$, corresponding to each site of the lattice initially occupied by a monomer. These equations have two remarkable features: they are (i) closed, and (ii) uncoupled (different masses not coupled). This empty interval method can be generalized to both spatially-inhomogeneous situations and monomer input. The solution can now be obtained by using the image method and gives $Q_n^k(t) = [I_{n-k}(2t) + I_{n+k}(2t)]e^{-2t}$. From this result, the cluster mass density $c_k = Q_1^k$ is

$$c_k(t) = [I_{k-1}(2t) - I_{k+1}(2t)]e^{-2t}. \tag{8.32}$$

Incidentally, the cluster densities are identical to the void densities (8.27), $c_k = V_{k+1}$. Intuitively, one may imagine that the entire mass in a void is contained by the cluster to its right.

Asymptotically, the cluster size distribution is

$$c_k(t) \simeq \frac{k}{\sqrt{\pi t^3/2}}\, e^{-k^2/2t}. \tag{8.33}$$

This distribution can be written in the scaling form, $c_k \sim t^{-1}\Phi(kt^{-1/2})$ with the scaling function (8.30). The scaled mass distribution differs significantly from the corresponding result for constant-kernel aggregation in the mean-field limit, $\Phi(z) = e^{-z}$ (see Eq. (3.9)). This mean-field result holds above the critical dimension $d > 2$. In one dimension there is a depletion of smaller than typical clusters $k \ll t^{1/2}$ and the decay at large masses is sharper, too: $\Phi(z) \sim e^{-z^2/2}$. Finally, notice that by summing the cluster mass distribution over all masses, we reproduce the density for coalescence, $c_{\rm coa} = c_1 + c_2 + c_3 + \ldots$. Similarly, by summing over odd sizes only, we reproduce the density for the annihilation case, $c_{\rm ann} = c_1 + c_3 + c_5 + \ldots$.

Aggregation with input

What happens when we now add monomers to the system at a constant rate? In our discussion of chapter 3 about aggregation with input in the mean-field limit, we found that a non-trivial steady state was created.

For the case of a constant reaction kernel, the steady-state mass distribution, $c_k(t \to \infty)$, had a $k^{-3/2}$ tail over a mass range $1 \ll k \ll t^2$. Our goal is to determine the corresponding behavior of steady-state aggregation in one dimension.

We first generalize the lattice description of aggregation by adding monomers to the system at a constant rate at each site: $0 \to A$ with rate h. In spite of this extra ingredient in the dynamics, it is still possible to write and solve the equations for the empty interval probabilities. The effect of input on the empty interval probability is quite simple: if an n interval contains mass $k-1$ and an input event occurs, there is a gain in Q_n^k. The rate at which mass is added to this interval is just $h\,n$; this is proportional to the interval size because input may occur at any of the sites. Similarly, if the interval contains mass k, input causes the loss of Q_n^k. Thus the master equation for Q_n^k is

$$\frac{dQ_n^k}{dt} = -2Q_n^k + Q_{n-1}^k + Q_{n+1}^k + h\,n\left[Q_n^{k-1} - Q_n^k\right]. \tag{8.34}$$

This equation holds for all $k > 0$ with the boundary condition $Q_n^{-1}(t) = 0$. While the equations are easy to formulate, the full time-dependent behavior is harder to obtain than in irreversible aggregation because the interval probabilities for different contained masses and different lengths are now all coupled.

However, the situation is much simpler in the steady state. In this case, we introduce the generating function, $Q_n(z) = \sum_k Q_n^k e^{kz}$, to convert Eq. (8.34) to

$$Q_{n-1}(z) + Q_{n+1}(z) = \left[2 + hn(1-e^z)\right] Q_n(z). \tag{8.35}$$

This recursion formula is the same as that for the Bessel function (Eq. (8.14)) when the index is properly matched. Thus following exactly the same line of reasoning as that leading to Eq. (8.15), The solution is now

$$Q_n(z) = \frac{J_{n+g^{-1}}(g^{-1})}{J_{g^{-1}}(g^{-1})}, \tag{8.36}$$

with $g \equiv g(z,h) = h(1-e^z)/2$. We are interested primarily in the large-k behavior of the mass distribution; this limit corresponds to the small-z behavior of the generating function. Thus we use the approximation $g \approx hz/2$ and the asymptotic formula (8.16) for the Bessel function to obtain

$$Q_1(z) \sim \frac{\mathrm{Ai}((2g)^{1/3})}{\mathrm{Ai}(0)} \sim 1 - \frac{\mathrm{Ai}'(0)}{\mathrm{Ai}(0)}(hz)^{1/3}. \tag{8.37}$$

This leading behavior $Q_1(z) = 1 - \text{const.} \times (hz)^{1/3}$ then implies an algebraic decay of the mass distribution

$$c_k \sim k^{-4/3}, \tag{8.38}$$

for $k \gg 1$. The exponent differs from the mean-field theory prediction (3.47), $c_k \sim k^{-3/2}$. Even though the mean-field theory fails quantitatively, it is still extremely valuable because it helps us articulate "what to expect". When there is input, mean-field theory predicted a power-law decay of the mass distribution for large masses, and this is what also occurs in one dimension. Similarly, for irreversible aggregation, mean-field theory predicts scaling behavior and a rapidly decaying tail of the mass distribution, again in qualitative accord with the behavior in one dimension.

Random River Networks

Aggregation with input is equivalent to the classic Scheidegger random river network model (Fig. 8.6). In this model, the downstream position along a river is equivalent to the time and the lateral meandering of a river is equivalent to a one-dimensional random walk. The source of a minimal size river is then equivalent to the injection of a unit mass. The meandering of a river is captured by a random walk and the merging of two rivers is equivalent to aggregation, as the flow rate of the combined rivers equals that of the two tributaries. The river network is therefore equivalent to the space-time diagram of aggregation with input. Let h be the river's depth. It's defining edges perform two independent random walks, so the river height distribution equals the first passage probability, $p(h) \sim h^{3/2}$. The river size k is proportional to the area of its drainage basin. The area scales as the depth times the height and since the width is diffusive ($\sim h^{1/2}$), the river size is $k \sim h \times h^{1/2} \sim h^{3/2}$. The size distribution

$$p(k) = p(s)\frac{ds}{dk} \sim k^{-4/3} \tag{8.39}$$

obtained from this heuristic argument therefore agrees with the asymptotic result (8.38).

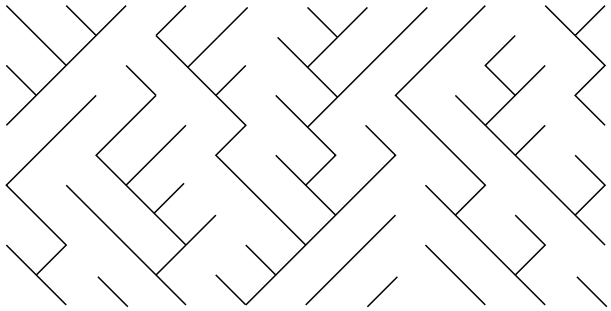

Figure 8.6: A river networks as aggregation with input. Shown are is the position versus time of the aggregates. This pictures depicts a "cellular automata" realization: a discrete time version where vacant site are immediately filled by particles. The lattice has been tilted by 45°.

8.4 Two Species Annihilation $A + B \to 0$

The reaction

$$A + B \to 0$$

is known as *two-species annhilation*. Here, same-species particles do not interact, while particles of the opposite species annihilate in pairs. Physical examples of this reaction include the annihilation of electron-hole pairs in a semiconductor or the annihilation of matter with antimatter in a cosmological setting. Perhaps the most striking aspect of diffusion-limited two-species annihilation is that the density decays as $t^{-d/4}$ for spatial dimension $d < 4$ for equal initial densities of the two species. This decay is much slower than the rate equation prediction of a t^{-1} decay and also slower than the $t^{-d/2}$ decay of single-species reactions for $d < 2$. The basic feature that gives rise to this anomalously slow kinetics is that the reactants organize into a coarsening mosaic of single-species domains (fig. 8.7). As a result, reactions can occur only near domain boundaries, rather than uniformly throughout the system. The inherent heterogeneity of the reaction leads to slow kinetics.

While the $t^{-d/4}$ density decay is has been proven by exact analysis methods, this approach involves mathematical techniques that lie outside the scope of this book. Thus in this chapter will primarily discuss qualitative approaches to determine the many interesting physical properties of two-species annihilation. While these approaches lack mathematical rigor, they are intuitive and easy to appreciate.

Density decay

Let us first give a back-of-the-envelope argument for the long-time behavior of the concentration $c(t)$ in terms of local density fluctuations. Consider a finite volume of linear dimension L. The number of particles of each species in this volume is given by

$$N_{A,B} = c(0)L^d \pm \sqrt{c(0)}\; L^{d/2}. \tag{8.40}$$

Here the $\pm$ in the second term signifies that, in a finite volume L^d, $N_{A,B}$ has fluctuations that are of the order of $\sqrt{c(0)}\; L^{d/2}$, in which the amplitude of this term is of order 1 and the sign that fluctuates from realization to realization. We now focus on the symmetric system where the two species are initially present in equal numbers. Then the initial difference in the number of A and B particles in the volume is

$$N_A - N_B \approx \pm\sqrt{c(0)}\; L^{d/2}. \tag{8.41}$$

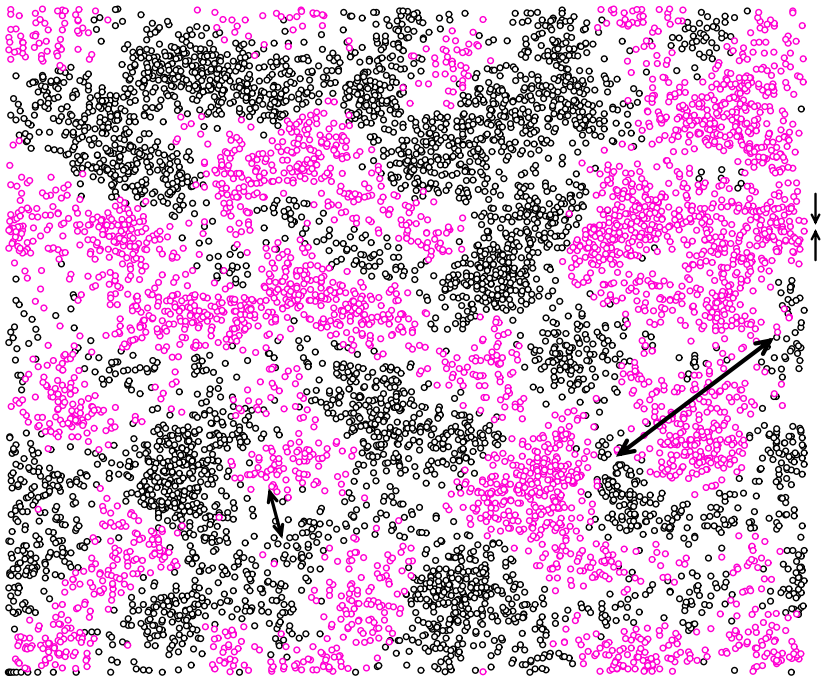

Figure 8.7: Snapshot of the particle positions in two-species annihilation in two dimensions, now showing the basic length scales of the system: the domain size, which scales as $t^{1/2}$, the interparticle spacing, which scales as $t^{1/4}$, and the depletion zone between domains, which scales as $t^{1/3}$ in two dimensions.

Roughly speaking, $N_A - N_B$ remains nearly constant during the time $t_L \sim L^2/D$ that it takes for a typical particle to traverse the volume by diffusion. After a time t_L, sufficient time has elapsed that particles have had time to annihilate with a member of the opposite species. Thus the "extensive" part of the particle number (the first term in Eq. (8.40)) will be eliminated, leaving behind the local majority species in the domain. By conservation of the difference of $N_A - N_B$, the number of particles in this local majority, $N_>(t_L)$, is of the order of is of order $\sqrt{c(0)}\, L^{d/2}$. Finally, by eliminating L in favor of t, we obtain

$$c(t) \approx N_>(t)/L^d \sim \sqrt{c(0)}\; (Dt)^{-d/4}, \qquad (d \leq 4). \tag{8.42}$$

Let us give a somewhat better grounded argument for anomalous $t^{-d/4}$ decay of the density by again focusing on the local density difference $\delta(\mathbf{r},t) \equiv c_A(\mathbf{r},t) - c_B(\mathbf{r},t)$. The concentration of each species evolves by the diffusion-reaction equation

$$\frac{\partial c_{A,B}(\mathbf{r},t)}{\partial t} = D\nabla^2 c_{A,B}(\mathbf{r},t) + R,$$

where R denotes the reaction term. We leave the reaction term unspecified because the density difference $\delta(\mathbf{r},t)$ evolves only by pure diffusion, $\frac{\partial\delta}{\partial t} = D\nabla^2\delta$. Consequently, the Fourier transform of the density difference is simply $\delta(\mathbf{k},t) = \delta(\mathbf{k},t=0)e^{-Dk^2t}$. At long times, there is minimal coexistence of A's and B's in the same spatial region because of the existence of domains. Thus $[c_A(\mathbf{r},t) - c_B(\mathbf{r},t)]^2 \approx 2c_A(\mathbf{r},t)^2$, so that

$$\begin{aligned}\int c_A(\mathbf{x},t)^2\, d\mathbf{x} &\approx \frac{1}{2}\int |\delta(\mathbf{k},0)|^2 e^{-Dk^2t}\, d\mathbf{k} \\ &\propto (Dt)^{-d/2}\int |\delta(\mathbf{q}/(Dt)^{1/2},t)|^2\, e^{-q^2}\, d\mathbf{q}. \end{aligned} \tag{8.43}$$

For a random initial condition, $|\delta(\mathbf{k},t=0)|^2 = N$ for all $\mathbf{k}$, since the mean-square involves the sum of N random unit vectors. Thus the integral over $\mathbf{q}$ in lasteq is independent of t, so that $\langle c_A(\mathbf{x},t)^2\rangle \sim \frac{N}{V}\,(Dt)^{-d/2}$. Finally the assumption of no cross correlations implies that $\langle c_A(\mathbf{x},t)^2\rangle \cong \langle c_A(\mathbf{x},t)\rangle^2$ and back 1 is reproduced. Notice that the random initial condition is a crucial aspect for obtaining the anomalous slow decay. In particular, for correlated initial conditions with no long-wavelength fluctuations in $\delta(\mathbf{x},t)$, the integral over $\mathbf{q}$ will vanish as $t \to \infty$, thus invalidating the above reasoning.

We conclude that a homogeneous system that is equally populated by A and B particles evolves into a continuously growing mosaic of single-species domains. The identity of each domain is determined by the local majority species in this same spatial region in the initial state. At time t, these domains will be of typical linear dimension $\sqrt{Dt}$, within which only the species in the local majority remains, with concentration $\sqrt{c(0)}\,(Dt)^{-d/4}$.

The spontaneous formation of domains breaks down for $d > 4$, however, because single-species domains become transparent to an invader of the opposite species. Consider, for example, the fate of a single A particle that is placed at the center of a B domain of linear dimension L and local concentration therefore of order $L^{-d/2}$. The impurity needs L^2 time steps to exit the domain, during which L^2 distinct sites will have been visited (again assuming $d > 4$). At each site, the A will react with probability of the order of the B concentration, $L^{-d/2}$. Therefore the probability that an A particle reacts with any B particle before exiting this domain is of order $L^{(4-d)/2}$. Since this probability vanishes as $L \to \infty$ when $d > 4$, a domain is unstable to diffusive homogenization and the system as a whole therefore remains spatially homogeneous.

Spatial organization

The above arguments suggest that two lengths are needed to characterize the reactant distribution in one dimension: the linear dimension of a typical domain, $L \propto (Dt)^{1/2}$, and the typical interparticle spacing, which scales as $c(t)^{-1} \propto t^{1/4}$. Surprisingly, there is yet another fundamental length scale in the system—the typical distance between and AB closest-neighbor pairs, ℓ_{AB}. The length ℓ_{AB} characterizes the gap that separates adjacent domains (Fig. 8.7). This gap is the fundamental control factor in the kinetics, since each reaction event involves diffusion of an AB pair across a gap.

To determine the evolution of ℓ_{AB}, let's first consider the simplest case of one dimension. We now reformulate the kinetics specifically in terms of the AB gap distance. Let c_{AB} denote the concentration of closest-neighbor AB pairs. Typical AB pairs react in a time $\Delta t \sim \ell_{AB}^2/D$. Since the number of reactions per unit length is of order c_{AB}, the rate of change of the overall concentration is

$$\frac{\Delta c}{\Delta t} \approx \frac{dc}{dt} \approx -\frac{c_{AB}}{\ell_{AB}^2/D}. \tag{8.44}$$

Now $\frac{dc}{dt}$ is known from $c(t)$ itself, while in one dimension, $c_{AB} \propto (Dt)^{-1/2}$, since there is one AB pair per domain of typical size $(Dt)^{1/2}$. Using these results and solving for ℓ_{AB} gives

$$\ell_{AB} \propto c(0)^{-1/4}\,(Dt)^{3/8}. \tag{8.45}$$

The fact that $\ell_{AB} \gg \ell_{AA}$ is a manifestation of the effective repulsion between opposite species. If one squints at Fig. 8.7, this inequality between ℓ_{AB} and ℓ_{AA} should be visually apparent.

The above results can be generalized to spatial dimension $1 \le d \le 2$. The time dependence of ℓ_{AB} still follows by applying (8.44), since it holds whenever random walks are compact (see the discussion in the

two paragraphs following Eq. (2.34) for a definition of compact random walks). We now assume that the interface of a single-species domain remains relatively smooth, so that a domain of linear dimension ℓ will interface of linear dimension $t^{(d-1)/2}$ and particles in the perimeter zone separated by a distance of the order of ℓ_{AB}, irrespective of identity, it is straightforward to obtain

$$\ell_{AB} \propto t^{(d+2)/[4(d+1)]}, \qquad c_{AB}(t) \propto t^{-d(d+3)/[4(d+1)]}, \tag{8.46}$$

which gives $\ell_{AB} \sim t^{1/3}$ and $c_{AB}(t) \sim t^{-5/6}$ in $d = 2$. For $d > 2$, the transience of random walks implies that two opposite species particles within a region of linear dimension ℓ_{AB} will react in a time of order ℓ_{AB}^d (rather than ℓ_{AB}^2). Consequently, (8.44) should be replaced by

$$\frac{\Delta c}{\Delta t} \approx -\frac{c_{AB}}{\ell_{AB}^d}. \tag{8.47}$$

This relation, together with the assumption of a smooth interfacial region between domains, gives, in $d > 2$ dimensions

$$\ell_{AB} \approx t^{d+2/[4(2d-1)]}, \qquad c_{AB} \approx t^{-d^2+5d-4/[4(2d-1)]}. \tag{8.48}$$

These coincide with (8.46) at $d = 2$, but yield $c_{AB} \approx t^{-1}$ and $\ell_{AB} \approx t^{1/4}$ for $d = 3$. The latter represents the limiting behavior where ℓ_{AB} becomes of the same order as ℓ_{AA}. Thus the non-trivial scaling of interparticle distances disappears in three dimensions and above.

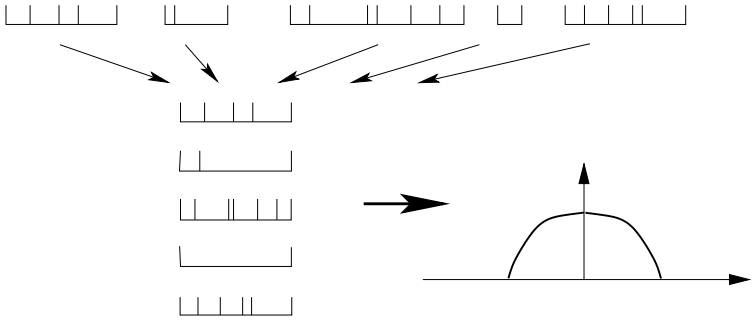

Figure 8.8: Construction of the microcanonical domain profile from the reactant positions (top line). Each domain is first scaled to a fixed length (lower left) and then their densities are superposed (lower right).

Much insight can be gained by studying the average density profile of a single domain. Consider the "microcanonical" density profile, $P^{(M)}(x)$, defined as the probability of finding a particle at a scaled distance x from the domain midpoint, when each domain is first scaled to a *fixed* size (Fig. 8.8). The resulting distribution is similar to the long-time probability distribution for pure diffusion in a fixed size absorbing domain. In contrast, for two-species annihilation, particles in a single domain are confined by absorbing boundaries which recede stochastically as $\sqrt{t}$ – the typical domain size. While the probability distribution inside such a stochastically evolving domain has not been solved, one can solve the related problem of a particle inside a deterministically growing domain $[-L(t), L(t)]$ with $L(t) \propto t^{1/2}$, The adiabatic approximation marginally applies in this case [16], and the density profile has the form $\cos(\pi x/L(t))$. This simple-minded modelling provides a useful framework to understand the domain profile in the reacting system.

Although determined by interactions between *opposite* species, this inhomogeneous domain profile governs the distribution of interparticle distances between *same* species. Particles are typically separated by a distance which grows as $t^{1/4}$ within the core of the domain, but systematically become sparser as the domain interface is approached. The subregions of "core" and "interface" each comprise a finite fraction of the domain. These essential features of the profile may be accounted for by the trapezoidal form (Fig. 2(b)),

$$\rho(z) \equiv c(x,t)\, t^{1/4} = \begin{cases} \rho_0, & |z| \le z^*; \\ \rho_0(1-|z|), & z^* < |z| < 1-\epsilon. \end{cases} \tag{8.49}$$

Here $z \equiv x/L(t)$ is the scaled spatial co-ordinate, with $x \in [-L(t), L(t)]$, and ρ_0 and $z^* \lesssim 1$ are constants. The upper limit for $|z|$ on the second line of lasteq reflects the fact that there are no particles within a scaled distance of $\epsilon \equiv \ell_{AB}/L(t) \sim t^{-1/8}$ from the domain edge. The linear decay of the concentration near the domain edge arises from the finite flux of reactants which leave the domain. Thus, the local nearest-neighbor distance is $\rho(z)^{-1}$, with $\rho(z) = \rho_0$ in the core ($|z| \leq z^*$), but with $\rho(z) = \rho_0(1 - |z|)$ near the boundary and the time dependence of the reduced moments of the AA distance distribution are

$$M_n \equiv \langle \ell_{AA}^n \rangle^{1/n} = \left(\int_0^\infty x^n \, P_{AA}(x,t)\, dx \right)^{1/n}, \tag{8.50}$$

$$\approx t^{1/4} \times \left(2\int_0^{z*} \frac{dz}{\rho_0^n} + 2\int_{z*}^{1-\epsilon} \frac{dz}{\rho_0^n (1-z)^n} \right)^{1/n}, \tag{8.51}$$

$$\sim \begin{cases} t^{1/4}, & n < 1; \\ t^{1/4} \ln t, & n = 1; \\ t^{(3n-1)/8n}, & n > 1. \end{cases} \tag{8.52}$$

For $n < 1$, the dominant contribution to M_n originates from the ρ_0^{-n} term in the parentheses, while for $n \geq 1$, the term involving $\rho_0^{-n}(1-z)^{-n}$ dominates, with the second term giving a logarithmic singularity at the upper limit for $n = 1$. Thus the large-scale modulation in the domain profile leads to moments $M_n(t)$ which are governed both by the gap length ℓ_{AB} and ℓ_{AA}. As $n \to \infty$, the reduced moment is dominated by the contribution from the sparsely populated region near the domain periphery where nearest-neighbor particles are separated by a distance of order $t^{3/8}$.

8.5 The Trapping Reaction $A + T \to T$

At first sight, the trapping reaction seems to be even simpler than annihilation or coalescence because trapping is essentially a single-particle problem. The system is populated by randomly-distributed static traps Fig. **??**. Static traps are randomly distributed in space and independent particles freely diffuse in this medium. Whenever a diffusing particle hits a trap it is immediately and permanently trapped. What is the probability $S(t)$ that a particle "survives" until time t?. At the most naive level, one might argue that one can replace any realization of the trapping medium by an effective average medium with a constant trapping rate. This would suggest that the density of survivors should decay exponentially with time. Surprisingly, this naive expectation is wrong and for interesting reasons. As we shall discuss, extreme fluctuations in the spatial distribution of traps in the form of large trap-free regions give rise to a slower decay of the survival probability. However, this anomalously slow decay manifests itself only when the density has decayed to an astronomically small value. One has to be careful to understand what may be of fundamental theoretical interest and what may be experimentally relevant.

Exact solution in one dimension

The essence of the problem can be appreciated already in one dimension where we can obtain the exact solution. A diffusing particle "sees" only the absorbing interval defined by the nearest surrounding traps. We can therefore adapt the solution for the concentration inside an absorbing interval $[0, L]$ (Chap. **??**) to determine the survival probability. For a particle initially at $x = x_0$, the concentration at time $t > 0$ is obtained from Eq. (**??**), with the coefficients A_n determined by matching the eigenfunction expansion to the initial condition. For a particle initially at x_0, A_n is thus given by the Fourier series inversion

$$c(x, t=0) = \delta(x - x_0) = \sum_{n=1}^{\infty} A_n \sin\left(\frac{n\pi x}{L}\right),$$

which gives

$$A_n = \frac{2}{L} \sin\left(\frac{n\pi x_0}{L}\right).$$

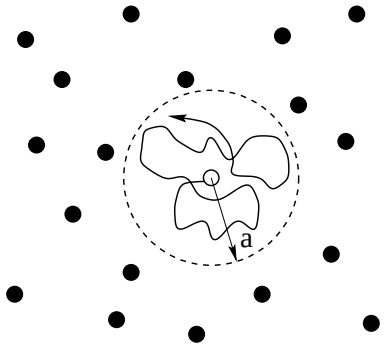

Figure 8.9: A configuration of traps (filled circles) and the trajectory of a diffusing particle. Also shown is the trap-free circle of radius a which is centered about the initial particle position. The probability that the particle remains in this circle is a lower bound for the exact particle survival probability in this configuration of traps.

Therefore the concentration within the interval is

$$c_L(x,t|x_0) = \frac{2}{L}\sum_{n=1}^{\infty} \sin\left(\frac{n\pi x}{L}\right)\, \sin\left(\frac{n\pi x_0}{L}\right)\; e^{-\left(\frac{n\pi}{L}\right)^2 Dt}. \tag{8.53}$$

For a fixed-length interval, we compute the survival probability by averaging over all initial particle positions and also integrating over all x. This gives

$$\begin{aligned}\overline{S_L(t)} &= \frac{1}{L}\int_0^L \int_0^L c_L(x,t|x_0)\, dx\, dx_0 \\ &= \frac{8}{\pi^2}\sum_{m=0}^{\infty} \frac{1}{(2m+1)^2}\; e^{-\frac{(2m+1)^2\pi^2}{L^2}Dt}.\end{aligned} \tag{8.54}$$

Next, we obtain the configuration-averaged survival probability by averaging this expression over the distribution of lengths of trap-free intervals. The simplest and most natural situation is a random distribution of traps at density ρ, for which the interval-length distribution is $P(L) = \rho e^{-\rho L}$. This gives the formal solution for the average survival probability

$$\begin{aligned}\langle S(t)\rangle &\equiv \langle \overline{S_L(t)}\rangle \\ &= \frac{8\rho}{\pi^2}\sum_{m=0}^{\infty} \frac{1}{(2m+1)^2}\int_0^{\infty}\; e^{-\frac{(2m+1)^2\pi^2}{L^2}Dt}\; e^{-\rho L}\, dL.\end{aligned} \tag{8.55}$$

As indicated in Fig. **??**, this integral has very different short- and long-time behaviors. In the former case, intervals of all lengths contribute to the survival probability, while at long times optimal-length intervals give the main contribution to the survival probability. This latter behavior is not visible until the survival probability has decayed to a vanishingly small and experimentally-unattainable value. In fact, the best strategy to observe the long-time behavior (by simulation) is to consider a system with a high concentration of traps (**?**)!

Long-time behavior

In the long-time limit, clearly the first term in the series for $\langle S(t)\rangle$ in Eq. (8.55) eventually dominates. If we retain only this term, it is relatively easy to determine the asymptotic behavior of the integral in Eq. (8.55). As a function of L, the first exponential factor in this equation rapidly increases to 1 as $L \to \infty$, while the second exponential factor decays rapidly with L. Thus the integrand has a peak as a function of L

which becomes progressively sharper as $t \to \infty$ (although this is not evident to the eye in Fig. **??**). We may therefore determine the asymptotic behavior of $\langle S(t)\rangle$ by the Laplace method (**?**).

To apply this method, we first rewrite Eq. (8.55) as $\langle S(t)\rangle \sim \int_0^\infty e^{f(L)}\, dL$, and then we fix the location of the maximum by defining the dimensionless length $\ell \equiv L/L^*$ to transform the integral to

$$\begin{aligned}\langle S(t)\rangle &= \frac{8\rho L^*}{\pi^2}\int_0^\infty \exp\left[-(\rho^2 Dt)^{1/3}[(\pi^2/2)^{2/3}\frac{1}{\ell^2} + (2\pi^2)^{1/3}\ell]\right]\, d\ell,\\ &\equiv \frac{8\rho L^*}{\pi^2}\int_0^\infty \exp\left[-(\rho^2 Dt)^{1/3}\, g(\ell)\right]\, d\ell. \end{aligned} \tag{8.56}$$

The integrand now has an increasingly sharp maximum at a fixed location as $t \to \infty$. We therefore expand $g(\ell)$ to second order about its maximum and perform the resulting Gaussian integral to obtain the leading behavior of $\langle S(t)\rangle$. From the condition that $g'(\ell^*) = 0$, we find $\ell^* = 1$, $g(\ell^*) = 3(\pi/2)^{2/3}$ and $g''(\ell^*) = -3\times(2\pi^2)^{1/3}$. Therefore

$$\begin{aligned}\langle S(t)\rangle &= \frac{8\rho L^*}{\pi^2}\int_0^\infty \exp\left[-(\rho^2 Dt)^{1/3}\, g(\ell)\right]\\ &\sim \frac{8\rho l^*}{\pi^2}\int_0^\infty \exp\left[-(\rho^2 Dt)^{1/3}\,[g(\ell^*) + \frac{1}{2}(\ell-\ell^*)^2 g''(\ell^*)]\right]\\ &\sim \frac{8\rho L^*}{\pi^2}\sqrt{\frac{2\pi}{(\rho^2 Dt)^{1/3}|g''(\ell^*)|}}\exp\left[-(\rho^2 Dt)^{1/3}\, g(\ell*)\right]\\ &= \frac{8\times 2^{2/3}}{3^{1/2}\pi^{7/6}}(\rho^2 Dt)^{-1/6}\,\exp(-3(\pi^2\rho^2 Dt/4)^{1/3}). \end{aligned} \tag{8.57}$$

The basic feature of this result is the relatively slow $e^{-t^{1/3}}$ asymptotic decay of $\langle S(t)\rangle$ compared to the exponential decay for the survival probability in a fixed-length interval. This slower decay stems from the contribution of optimal intervals whose length ℓ^* grows as $t^{1/3}$. Although such large intervals are rare, their contribution to the survival probability is asymptotically dominant. In Subsection 8.5.0.1, we shall see how these extreme intervals are the basis for the Lifshitz tail argument which provides the asymptotic decay of $\langle S(t)\rangle$ in arbitrary spatial dimension. Finally, if one is interested in only the correct controlling factor in the asymptotic survival probability, one can merely evaluate $f(L)$ at its maximum of $L^*(t) = (2\pi^2 Dt/\rho)^{1/3}$ and then estimate $\langle S(t)\rangle$ as $e^{f(L^*)} \sim e^{-\text{const.}\times(\rho^2 Dt)^{1/3}}$.

8.5.0.1 Short-Time Behavior

It is instructive to study the short-time behavior of $\langle S(t)\rangle$, both because the time dependence is interesting and because this limit indicates that the crossover to the asymptotic behavior for $\langle S(t)\rangle$ is very slow. In fact, the asymptotic decay does not arise until the density has decayed to an extremely small value. Thus although there is considerable theoretical appeal in understanding the long-time decay of the trapping reaction, its practical implications are limited.

There are many ways to estimate the short-time behavior. One crude approach is to notice that, at early times, the factor e^{-Dt/L^2} reaches 1 as a function of L (at $L \approx \sqrt{Dt}$) before there is an appreciable decay in the factor $e^{-\rho L}$ (at $L \approx 1/\rho$). Thus to estimate $\langle S(t)\rangle$, we may cut off the lower limit of the integral at $\sqrt{Dt}$ and replace the factor e^{-Dt/L^2} by 1 (see Fig. **??**). Using this approximation, the time dependence of the survival probability is

$$\begin{aligned}\langle S(t)\rangle &\approx \int_{\sqrt{Dt}}^\infty e^{-\rho L}\, dL\\ &\approx e^{-\text{const.}\times\rho\sqrt{Dt}}. \end{aligned} \tag{8.58}$$

This short-time behavior extends until $t \sim 1/(D\rho^2)$, which translates to the diffusion distance being of the order of the mean separation between traps.

A more rigorous approach is to use the fact we should keep all the series terms in Eq. (8.55). As shown in Weiss' book (**?**), this series can be evaluated easily by defining $\epsilon = \pi^2 Dt/L^2$ and noting that $dS/d\epsilon$ has the form

$$\left\langle \frac{\partial S(t)}{\partial \epsilon} \right\rangle = \frac{8\rho}{\pi^2} \int_0^\infty \left(\sum_{m=0}^{\infty} e^{-(2m+1)^2 \epsilon} \right) e^{-\rho L}\, dL.$$

We can estimate the sum by replacing it with an integral, and then we can easily perform the average over L, with the result

$$\langle S(t) \rangle \sim e^{-\rho\sqrt{8Dt/\pi}}. \tag{8.59}$$

Now we may roughly estimate the crossover between the short- and the long-time limits by equating the exponents in Eqs. (8.57) and (8.59). This gives the numerical estimate $\rho^2\, Dt \approx 269$ for the crossover time. Substituting this into the above expression for the short-time survival probability shows that $\langle S(t) \rangle$ must decay to approximately 4×10^{-12} before the long-time behavior represents the main contribution to the survival probability. In fact, because of the similarity of the short- and the long-time functional forms, the crossover is very gradual, and one must wait much longer still before the asymptotic behavior is clearly visible. Although this discussion needs to be interpreted cautiously because of the neglect of the power-law factors in the full expressions for the survival probability, the basic result is that the asymptotic survival probability is of marginal experimental utility. In spite of this deficiency, the question about the asymptotic regime is of fundamental importance, and it helps clarify the role of exceptional configurations in determining the asymptotic survival probability.

Lifshitz Argument for General Spatial Dimension

In higher dimensions, it is not possible to perform this average directly. As a much simpler alternative, we will apply a Lifshitz argument to obtain the asymptotic behavior of the survival probability. Part of the reason for presenting this latter approach is its simplicity and wide range of applicability. One sobering aspect, however, is that the asymptotic survival probability does not emerge until the density has decayed to an astronomically small value. Such a pathology typically arises when a system is controlled by rare events. This serves as an important reality check for the practical relevance of the Lifshitz argument.

The Lifshitz approach has emerged as an extremely useful tool to determine asymptotic properties in many disordered and time-varying systems **?**. If we are interested *only* in asymptotics, then it is often the case that a relatively small number of extreme configurations provide the main contribution to the asymptotics. The appeal of the Lifshitz approach is that these extreme configurations are often easy to identify and the problem is typically straightforward to solve on these configurations.

In the context of the trapping reaction, we first identify the large trap-free regions which give the asymptotically dominant contribution to the survival probability. Although such regions are rare, a particle in such a region has an anomalously long lifetime. By optimizing the survival probability with respect to these two competing attributes, we find that the linear dimension of these extreme regions grows as $(Dt)^{1/(d+2)}$ for isotropic diffusion, from which we can easily find the asymptotic survival probability.

8.5.0.2 Isotropic Diffusion

It is convenient to consider with a lattice system in which each site is occupied by a trap with probability p and in which a single particle performs a random walk on free sites. The average survival probability $\langle S(t) \rangle$ is obtained by determining the fraction of random-walk trajectories which do not hit any trap up to time t. This fraction must be averaged over all random-walk trajectories *and* over all trap configurations.

An important aspect of these averages is that they may be performed in either order, and it is more convenient to first perform the latter. For a given trajectory, each visited site must not be a trap for the particle to survive, while the state of the unvisited sites can be arbitrary. Consequently, a walk which has visited s *distinct* sites survives with probability q^s, with $q = (1 - p)$. Then the average survival probability is

$$\langle S(t) \rangle = z^{-N} \sum_s C(s,t) q^s \equiv \langle q^s \rangle, \tag{8.60}$$

where $C(s,t)$ is the number of random walks which visit s distinct sites at time t and z is the lattice coordination number. Notice that the survival probability is an exponential-order moment of the distribution of visited sites. It is this exponential character which leads to the anomalous time dependence of the survival probability.

Clearly the survival probability for each configuration of traps is bounded from below by the contribution which arises from the *largest* spherical trap-free region centered about the initial particle position (Fig. 8.9). This replacement of the configurational average by a simpler set of extremal configurations is the essence of the Lifshitz tail argument. The probability for such a region to occur is simply q^V, where $V = \Omega_d r^d$ is the number of sites in this d-dimensional sphere of radius r. We determine the probability for a particle to remain inside this sphere by solving the diffusion equation with an absorbing boundary at the sphere surface. This is a standard and readily-soluble problem, and the solution is merely outlined.

Since the system is spherically symmetric, we separate the variables as $c(r,t) = g(r)f(t)$ and then introduce $h(r) = r^\nu g(r)$, with $\nu = \frac{d}{2} - 1$ to transform the radial part of the diffusion equation into the Bessel differential equation

$$h''(x) + \frac{1}{x}h'(x) + \left(1 - \frac{1}{x^2}\left(\frac{d}{2} - 1\right)^2\right) h(x) = 0,$$

where $x = r\sqrt{k/D}$, the prime denotes differentiation with respect to x, and the boundary condition is $h(a\sqrt{k/D}) = 0$, where a is the radius of the trap-free sphere. Correspondingly $f(t)$ satisfies $\dot{f} = -kf$. In the long-time limit, the dominant contribution to the concentration arises from the slowest decaying mode in which the first zero of the Bessel function $J_{d/2}(r\sqrt{k/D})$ occurs at the boundary of the sphere. Thus the survival probability within a sphere of radius a asymptotically decays as

$$S(t) \propto \exp\left(-\frac{\mu_d^2 Dt}{a^2}\right),$$

where μ_d is the location of the first zero of the Bessel function in d dimensions.

To obtain the configuration-averaged survival probability, we average this survival probability for a fixed-size sphere over the radius distribution of trap-free spheres. This gives the lower bound for the average survival probability,

$$\langle S(t)\rangle_{\rm LB} \propto \int_0^\infty \exp\left[-\frac{\mu_d^2 Dt}{r^2} + \Omega_d r^d \ln q\right] r^{d-1}\, dr. \tag{8.61}$$

This integrand becomes sharply peaked as $t \to \infty$, and we can again estimate the integral by the Laplace method. As in one dimension, we rescale variables to fix the location of the maximum. Writing the integrand in Eq. (8.61) as $\exp[-F(r)]$ and differentiating with respect to r, we find that the maximum of F occurs at

$$r^* = \left(-\frac{2\mu_d^2 Dt}{\Omega_d d \ln q}\right)^{1/(d+2)}.$$

This defines the radius of the trap-free region which gives the dominant contribution to the survival probability at time t. We now rewrite F in terms of the scaled variable $u = r/r^*$ to give

$$F(u) = -(\mu_d^2 Dt)^{d/(d+2)}(-\Omega_d \ln q)^{2/(d+2)}\left[\left(\frac{d}{2u}\right)^{2/(d+2)} + \left(\frac{2u}{d}\right)^{d/(d+2)}\right].$$

We now evaluate the integral by expanding $F(u)$ to second order in u and performing the resulting Gaussian. This gives, for the controlling exponential factor in the average survival probability,

$$\begin{aligned}\langle S(t)\rangle_{\rm LB} &\propto \exp\left[-\text{const.} \times (Dt)^{d/(d+2)}(\ln w)^{2/(d+2)}\right] \\ &\equiv \exp[-(t/\tau)^{2/(d+2)}].\end{aligned} \tag{8.62}$$

There are two noteworthy points about this last result. First, this type of stretched exponential behavior is not derivable by a classical perturbative expansion, such as an expansion in the density of traps. Second,

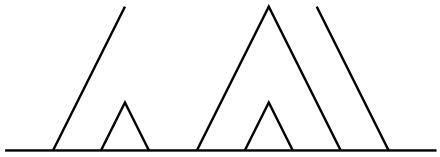

Figure 8.10: Ballistic annihilation with two-velocities.

as in the case of one dimension, the asymptotic decay in Eq. (8.62) again does not set in until the density has decayed to an astronomically small value. We can again obtain a rough estimate for this crossover time by comparing the asymptotic survival probability with the survival probability in the short-time limit. A cheap way to obtain the latter is to expand Eq. (8.60) as $\langle q^s\rangle = \langle 1 + s\ln q + (s\ln q)^2/2 + \ldots\rangle$, retain only the first two terms, and then re-exponentiate. This then gives

$$\langle S(t)\rangle_{\text{short time}} \approx q^{\langle s\rangle} \to e^{-\rho D t\, a^{d-2}}, \tag{8.63}$$

where a is the lattice spacing and we have assumed the limit of a small concentration of traps. By comparing the asymptotic form Eq. (8.62) with the short-time approximation of (8.63), we can infer the crossover time between short-time and asymptotic behavior and then the value of the survival probability at this crossover point. The detailed numerical evaluation of these numbers is tedious and unenlightening; however, the basic result is that the survival probability begins to show its asymptotic behavior only after it has decayed to a microscopically small value. In fact, the crossover to asymptotic behavior occurs earliest when the concentration of traps is large. This is counter to almost all simulation studies of the trapping reaction.

8.6 Ballistic Annihilation

In ballistic annihilation, particles move at constant velocity and annihilation occurs whenever two particles meet.

We start we the case of bimodal velocity distributions. The two velocies can be taken to be equal in magnitude and opposite in sign: v_0 and $-v_0$. The concentration of the two particles are equal c_0.

The two-velocity problem is analytically tractable because it maps directly to the survival probability of a random walk in the presence of a trap. As in the traffic problem, a positive velocity particle is of course affected only by particles ahead of it. Its collision partner depends only on the velocities of the particles ahead but not on their actual positions. For the velocity configuration be $++-+++---\cdots$, the 0th particle is bound to collide with the 7th particle (Fig.8.10). In general, it collides with the kth particle when the velocity sum $\sum_{i=0}^{m} v_i \geq 0$ for all $m < 2k$ but $\sum_{i=0}^{2k+1} v_i < 0$.

Let p_k the probability that $2k$ consecutive particles all annihilate among themselves. Manually, we find $p_0 = 1$, $p_1 = 1/4$ and $p_2 = 1/8$. This probability satisfies the recursion relation

$$p_k = \frac{1}{4}\sum_{j=1}^{k-1} p_j p_{k-1-j} \tag{8.64}$$

for $k > 0$ with $p_0 = 1$. The generating function $p(z) = \sum_{k=0}^{\infty} p_k z^k$ satisfies $\frac{z}{4}P^2(z) - P(z) + 1 = 0$. Its solution, $p(z) = 1 - \sqrt{1-z}$ yields the probabilities

$$p_k = 4^{-k}\frac{(2k)!}{k!(k+1)!}. \tag{8.65}$$

These probabilities allow calculation of the density of remaining particles for arbitrary spatial distributions. For simplicity, we consider a regular array of particles, with spacing all equal to $1/c_0$. For a positive particle to survive to time t it must be destined to collide with a particle of index $k > c_0 v_0 t$. Therefore, the particle concentration equals $c(t) = c_0 \sum_{k>c_0 v_0 t} p_k$. Using $p_k \sim k^{-3/2}$ leads to the concentration decay

$$c(t) \sim \left(\frac{c_0}{v_0 t}\right)^{1/2}. \tag{8.66}$$

Thus, the concentration decays algebraically with time, much slower compared with the exponential decay for traffic with bimodal velocity distributions. Moreover, the concentration depends on the initial condition (there is an explicit dependence on the initial concentration) in contrast with the single-species annihilation decay (8.2).

The long time behavior is dominated by fluctuations in the initial conditions, a behavior that is in some sense similar to both the traffic problem and the two-species annihilation reaction in low spatial dimensions. We employ the finite-size scaling argument (see box in chapter 7). In a finite system, there are initially N_+ and N_- particles with $N_+ + N_- = c_0 L$. The fluctuations in the particle numbers are characterized by the number difference $\Delta N = |N_+ - N_-|$ and since the initial concentrations are the same, this fluctuation grows diffusively with the total particle number $\Delta N \sim N^{1/2}$. The final state consists of all the excess majority particles, so $c(L) \sim \Delta/L \sim (c_0/L)^{-1/2}$. Since the only dynamical scale in the problem is the ballistic scale $v_0 t$ we anticipate that the time dependent concentration obeys the scaling relation $c(L,t) \sim (c_0 L)^{-1/2}\Phi(tv_0/L)$. In the infinite system size limit, the concentration should depend on time alone so $\Phi(z) \sim z^{-1/2}$ as $z \to 0$ therefore reproducing (8.66).

A rich behavior occurs when there are three types of velocities. In the symmetric case of three velocities $-v_0$, 0, and v_0 with equal concentrations of mobile particles, $c_+(0) = c_-(0)$ and $c_0(0) = 1 - c_-(0) - c_+(0)$, there is a phase transition at $c_0(0) = 1/4$. The problem reduces to the two-velocity case when $c_0(0) < 1/4$ with the mobile concentration decaying as $c_\pm(t) \sim t^{-1/2}$ and the immobile concentration decaying as $c_- \sim t^{-1}$. At the critical point, all the concentrations decay asymptotically as $t^{-2/3}$. Above the critical concentration, a finite fraction of the immobile particles survive, and the mobile particle concentration decays exponentially with time.

For continuous velocity distributions, the behavior is qualitatively similar to traffic flows. The velocity decays as $v \sim t^{-\beta}$ and the concentration as $c \sim t^{-\alpha}$. From dimensional analysis the exponent relation $\alpha + \beta = 1$ holds. The exponents vary continuously with the parameter μ in (13.66). The exponents values $\beta(\mu)$ differ from the traffic case, but qualitatively, they do exhibit a similar dependence on μ. Overall, the Boltzmann equation

$$\frac{\partial P(v,t)}{\partial t} = -P(v,t)\int_{-\infty}^{\infty} dv' |v - v'| P(v',t) \tag{8.67}$$

provides a decent approximation. For example, it predicts $\beta(0) = 0.230472$ compared with Monte Carlo simulation results $\beta = 0.196$.

Combining the results for traffic flows, ballistic agglomeration, and ballistic annihilation, we conclude that reaction processes with a ballistic transport are much less robust compared with their diffusive counterparts. Dimensional analysis is generally inappropriate for describing the behavior as exponents can be transcendental. Conservations laws play an important role. The notion of universality classes is also not too useful. While the most complete knowledge was obtained for the exactly solvable traffic model, exact solutions are very difficult and generally require different techniques for different problems.

References

1. Ya. B. Zeldovich and A. A. Ovchinnikov, Chem. Phys. **28**, 215 (1978).
2. D. Toussaint and F. Wilczek, J. Chem. Phys. **78**, 2642 (1983).
3. Z. Rácz, Phys. Rev. Lett. **55**, 1707 (1985).
4. K. Kang and S. Redner, Phys. Rev. A **32**, 435 (1985).
5. A. A. Lushnikov, JETP **64**, 811 (1986).
6. J. L. Spouge, Phys. Rev. Lett. **60**, 871 (1988).
7. H. Takayasu, I Nishikawa, and H. Tasaki, Phys. Rev. A **37**, 3110 (1988).
8. B. R. Thomson, J. Phys. A **22**, 879 (1989).
9. J. G. Amar and F. Family, Phys. Rev. A **41**, 3258 (1990).

10. D. ben-Avraham, M. A. Burschka, and C. R. Doering, J. Stat. Phys. **60**, 695 (1990).
11. B. Derrida, C. Godrèche, and I. Yekutieli, Phys. Rev. A **44**, 6241 (1991).
12. M. Bramson and J. L. Lebowitz, J. Stat. Phys. **65**, 941 (1991).
13. F. Leyvraz and S. Redner, Phys. Rev. A **46**, 3132 (1992).
14. B. Derrida, A. J. Bray and C. Godrèche, J. Phys. A **27**, L357 (1994).
15. B. Derrida, V. Hakim, and V. Pasquier, Phys. Rev. Lett. **75**, 751 (1995).
16. S. N. Majumdar, A. J. Bray, C. Cornell, and C. Sire, Phys. Rev. Lett. **77**, 3704 (1996).

9.4 Ballistic Anihilation

17. Y. Elskens and H. L. Frisch, Phys. Rev. A **31**, 3812 (1985).
18. E. Ben-Naim, S. Redner, and F. Leyvraz, Phys. Rev. Lett. **70**, 1890 (1993).
19. P. L. Krapivsky, S. Redner, and F. Leyvraz, Phys. Rev. E **51**, 3977 (1995).
20. P. L. Krapivsky and C. Sire, Phys. Rev. Lett. **86**, 2494 (2001).